High-resolution ghost imaging through complex scattering media via a temporal correction

YIN XIAO,[1] LINA ZHOU,[1] AND WEN CHEN[1,2,*]

[1]*Department of Electronic and Information Engineering, The Hong Kong Polytechnic University, Hong Kong, China*
[2]*Photonics Research Institute, The Hong Kong Polytechnic University, Hong Kong, China*
Corresponding author: owen.chen@polyu.edu.hk

In this letter, we propose high-resolution ghost imaging (GI) through complex scattering media using temporal correction. We provide evidence that theoretical description about the GI based on spatially correlated beams is still incomplete and cannot work in complex scenarios. We complete the description of temporal correction of beam correlations in the GI. The optical experiments demonstrate that high-resolution ghost images can always be retrieved by using the rectified temporally-corrected beam correlation algorithm even in complex, dynamic and highly strong scattering environments where conventional GI totally cannot work. By using the proposed method, quality of the retrieved ghost images through complex scattering media can be enhanced effectively as the number of realizations increases, which cannot be achieved by conventional GI. The established general framework provides optical insights beyond the current understanding of GI, and the rectified theory and experimental results would represent a key step towards applications of the GI over a wide range of free-space wave propagation environments.

Ghost imaging (GI) was studied and applied to retrieve sample information based on spatially correlated beams [1]. In the GI, the illumination beam is split into two beam paths. One beam illuminates a sample collected by using a single-pixel bucket detector without spatial resolution, and transverse distribution of another beam never interacting with the sample is collected by using a pixelated detector. Spatial properties of the sample can be retrieved using a correlation operation between the spatially correlated beams. There is either quantum or classical correlation involved in the GI [2]. In quantum optics, the GI is created with correlated beams of entangled photons, and is developed based on quantum entanglement proposed by Klyshko [3]. Shih and coworkers [4] developed the GI using entanglement photon pairs generated from spontaneous parametric down-conversion. Although quantum-entanglement-based GI has been theoretically and experimentally verified, it was found that quantum

entanglement was not compulsory to be applied in the GI to retrieve ghost images. Therefore, classical GI using pseudo-thermal light has been further developed [5].

In the GI, different light sources have been studied and applied, e.g., X-ray [6], Terahertz [7], cold atom [8], electron [9] and neutron [10]. The extension and studies are significant for the development of GI. For instance, X-ray GI could reduce dose rate of radiation used in the imaging and tomography [11]. Computational GI (CGI) [12] has also been developed which simplifies the GI setup with only one beam path by explicitly controlling the distribution of incident illumination using a spatial light modulator.

The GI could outperform 2D pixelated-detector-based imaging approaches in many situations, e.g., absorbing samples [13], low light intensities [14] and scattering media [15]. The GI method has been employed in various fields, e.g., three-dimensional imaging [16], cytometry [17], encryption [18], telecommunications [19], remote sensing [20] and pattern recognition [21]. The modified GI algorithms [22,23] have also been studied and applied for a purpose of finding novel applications and retrieving ghost images with improved signal-to-noise ratio (SNR). Although second-order correlation algorithm has been investigated in the GI, it is not a completely theoretical description. In optical channel of the GI, scaling factors exist physically and can play an important role. The GI based on spatially correlated beams always considers scaling factors as a constant, which may not be fully feasible. The second-order correlation algorithm is not generally feasible and efficient for the GI to work in various free-space wave propagation environments, and it is always desirable to complete theoretical description about the GI in order to establish a general framework.

In this letter, we propose high-resolution temporally-corrected GI (TCGI) through complex scattering media. We provide evidence that theoretical description about the GI based on spatially correlated beams is still incomplete and cannot work in complex scenarios. We complete the description of temporal correction of beam correlations in the GI. The proposed TCGI takes scaling factors into consideration, and a theoretical derivation about the GI is completely described. In the proposed TCGI, a temporal carrier is introduced and used to correct scaling factors physically existing in the imaging channel. High-resolution ghost images can always be retrieved by using the proposed TCGI even in complex, dynamic

and highly strong scattering environments where conventional GI totally cannot work. The rectified correlation algorithm in the proposed TCGI provides a general framework and optical insights beyond the current understanding of GI, and gives rise to applications of the GI over a wide range of free-space wave propagation environments.

When scaling factors physically existing in the GI are taken into consideration, single-pixel detection process in various free-space wave propagation environments in the GI can be described by

$$B = k \int I(\mathbf{x}) G(\mathbf{x}) d\mathbf{x}, \tag{1}$$

where B denotes single-pixel value (i.e., a realization in the GI), k denotes scaling factor in optical channel, $I(\mathbf{x})$ denotes an illumination pattern with spatial coordinate $\mathbf{x}$, and $G(\mathbf{x})$ denotes intensity transmission function of a sample. Then, the correlation operation between intensity fluctuation δB and $\delta I(\mathbf{x})$ can be described by

$$O(\mathbf{x}) = \langle \delta B \delta I(\mathbf{x}) \rangle = \langle (B - \langle B \rangle)(I(\mathbf{x}) - \langle I(\mathbf{x}) \rangle) \rangle, \tag{2}$$

where $O(\mathbf{x})$ denotes a retrieved ghost image, $\langle \rangle$ denotes an ensemble averaging over the total number of realizations, $\delta B = B - \langle B \rangle$, and $\delta I(\mathbf{x}) = I(\mathbf{x}) - \langle I(\mathbf{x}) \rangle$.

The scaling factors physically existing in the GI are always assumed as a constant which has no any effect on the correlation algorithm in Eq. (2). Since scattering or turbulence, e.g., complex and dynamic, is a significant challenge in the GI, scaling factors in optical channel could be severely modified. A direct calculation of $\langle B \rangle$ and δB could be physically meaningless due to the variation of scaling factors, e.g., through dynamic and strong scattering media. Therefore, the correlation algorithm is not generally feasible and effective for the retrieval of ghost images in many application scenarios. It is crucial to investigate the variation of scaling factors physically existing in the optical channel and completely derive second-order correlation algorithm to establish a general framework for the GI.

To solve the problem induced by the variation of scaling factors physically existing in the GI, a temporal carrier $T(\mathbf{x})$ is introduced (see Section 1 in Supplement 1 for the details) in this study and used before each illumination pattern $I(\mathbf{x})$. When the fixed temporal carrier and each illumination pattern are alternately used to sequentially illuminate a sample in the GI, single-pixel detection process is respectively described by

$$B_{ti} = k_{ti} \int T(\mathbf{x}) G(\mathbf{x}) d\mathbf{x}, \tag{3}$$

$$B_i = k_i \int I_i(\mathbf{x}) G(\mathbf{x}) d\mathbf{x}, \tag{4}$$

where i denotes a sequence (i.e., 1,2,3,...), B_{ti} denotes the single-pixel intensity values corresponding to temporal carrier $T(\mathbf{x})$, k_{ti} denotes scaling factors corresponding to the temporal carrier, B_i denotes the single-pixel intensity value corresponding to each illumination pattern $I_i(\mathbf{x})$, and k_i denotes scaling factors corresponding to the illumination patterns. Since the time interval

between the fixed temporal carrier $T(\mathbf{x})$ and each illumination pattern $I_i(\mathbf{x})$ embedded into a spatial light modulator is short, a relationship of $k_{ti} \approx k_i$ can be employed. Therefore, scaling factors in the GI can be eliminated by using the recorded single-pixel intensity values corresponding to the temporal carrier, which is described by

$$\frac{B_i}{B_{ti}} \approx \frac{\int I_i(\mathbf{x}) G(\mathbf{x}) d\mathbf{x}}{\int T(\mathbf{x}) G(\mathbf{x}) d\mathbf{x}}. \tag{5}$$

Here, a fixed temporal carrier $T(\mathbf{x})$ is used before each illumination pattern $I_i(\mathbf{x})$. The denominator in Eq. (5) can be considered as a constant ρ described by

$$\rho = \int T(\mathbf{x}) G(\mathbf{x}) d\mathbf{x}. \tag{6}$$

Then, we have

$$\int I_i(\mathbf{x}) G(\mathbf{x}) d\mathbf{x} \approx \rho \frac{B_i}{B_{ti}}. \tag{7}$$

The left part in Eq. (7) represents the sum of a product between each illumination pattern $I_i(\mathbf{x})$ and intensity transmission function of the sample. After $\int I_i(\mathbf{x}) G(\mathbf{x}) d\mathbf{x}$ is denoted as B_i', we have

$$B_i' \approx \rho \frac{B_i}{B_{ti}}. \tag{8}$$

Different from the resultant B in Eq. (1), B_i' in Eq. (8) does not contain the impact of scaling factors physically existing in optical channel of the GI. The result obtained in Eq. (8) is further used in correlation algorithm, and a wide range of free-space wave propagation environments, e.g., through complex, dynamic and highly strong scattering media, can be studied. Applying Eq. (8) into Eq. (2), we have

$$O(\mathbf{x}) = \left\langle \left(\rho \frac{B_i}{B_{ti}} - \left\langle \rho \frac{B_i}{B_{ti}} \right\rangle \right) \left(I_i(\mathbf{x}) - \langle I_i(\mathbf{x}) \rangle \right) \right\rangle. \tag{9}$$

Since ρ is a constant that has no any effect, it can be omitted. Equation (9) can be re-written as

$$O(\mathbf{x}) = \left\langle \left(\frac{B_i}{B_{ti}} - \left\langle \frac{B_i}{B_{ti}} \right\rangle \right) \left(I_i(\mathbf{x}) - \langle I_i(\mathbf{x}) \rangle \right) \right\rangle. \tag{10}$$

The rectified correlation algorithm in Eqs. (9) and (10) provides a general framework for the GI, and can be used for the retrieval of high-resolution ghost images in various free-space wave propagation environments, e.g., imaging without scattering media in free space and through complex and dynamic scattering media where conventional GI methods totally cannot work.

To verify the rectified correlation algorithm in the proposed TCGI, a series of optical experiments are conducted to realize the retrieval of high-resolution ghost images in complex scenarios. In Fig. 1, a green laser with power of 25.0 mW and wavelength of 532.0 nm is used. A series of 2D random amplitude-only patterns with 128×128 pixels are generated, and are sequentially embedded into an amplitude-only spatial light modulator

(Holoeye, LC-R720) with pixel size of 20.0 μm. The fixed temporal carrier and each illumination pattern are alternately embedded into the amplitude-only spatial light modulator. 38000 random amplitude-only illumination patterns are used in this study as a typical example, and the fixed temporal carrier, i.e., a pre-generated random amplitude-only pattern, is used before each illumination pattern. USAF 1951 resolution target is used as a sample in the experimental setup, and imaging through complex, dynamic and highly strong scattering media is studied. It is worth noting that the amplitude-only patterns are projected onto the sample by using a 4f system, which is not shown in Fig. 1. In the water tank (transparent polymethyl methacrylate) with dimensions of 10.0 cm (L) × 30.0 cm (W) × 30.0 cm (H), clean water of 6000 ml is first placed. Then, in the imaging process, skimmed milk (total volume of 10.0 ml) keeps dropping into the water tank over 102.0 minutes. To create a dynamic environment, a stirrer is used to operate at 500.0 rpm. A single-pixel bucket detector (Thorlabs, PDA100A2) is used to record a series of intensity values. In optical experiments, axial distance between water tank and the single-pixel detector is 22.0 cm, and axial distance between the sample and the single-pixel detector is 42.0 cm.
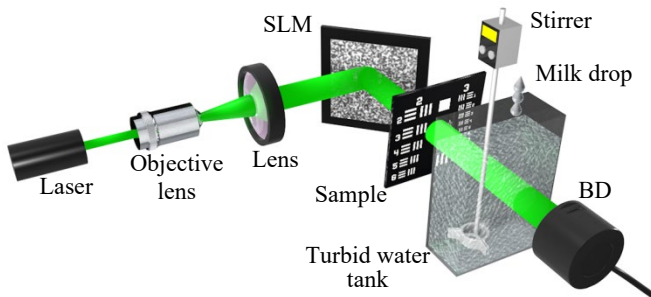

Fig. 1. Schematic of an optical setup in complex, dynamic and highly strong scattering media to verify the rectified correlation algorithm in the proposed TCGI. SLM: Spatial light modulator; BD: Bucket detector. The USAF 1951 resolution target is used as a sample.

The free-space wave propagation environment in Fig. 1 changes characteristics of optical channel in the single-pixel measurement process. Supposed that only the realizations corresponding to the series of illumination patterns are used based on spatially correlated beams in Eq. (2), it is impossible to retrieve information of the sample. The ground truth is shown inside red box in Fig. 2(a), and the retrieved result based on Eq. (2) is shown in Fig. 2(b). It can be seen in Fig. 2(b) that no information about the sample can be retrieved even when 38000 realizations are used. Experimental results demonstrate that theoretical description in the GI is incomplete, and cannot provide a general framework for the retrieval of ghost images in various free-space wave propagation environments. When the realizations measured corresponding to the series of illumination patterns and the fixed temporal carrier are employed in Eq. (10) in the proposed TCGI, experimental result is shown in Fig. 2(c). It can be seen that a high-resolution ghost image is retrieved, and spatial resolution of 70.15 μm (i.e., element 6 of group 2 in USAF 1951 resolution target) is achieved. The spatial resolution achieved is close to theoretical

limit in this GI system. Experimental results in Fig. 2 verify the rectified correlation algorithm in the proposed TCGI.
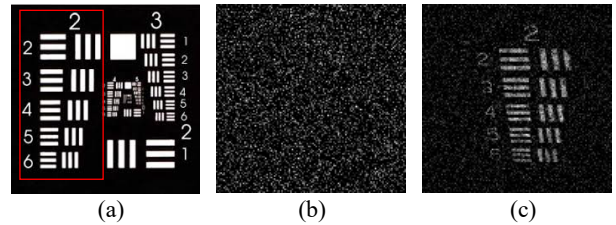

Fig. 2. (a) Ground truth (i.e., the part inside red box), (b) a retrieved ghost image using the GI with 38000 realizations, and (c) a retrieved ghost image using the rectified correlation algorithm in the proposed TCGI with 38000 realizations. The retrieved ghost image is slightly tilted due to the illumination angle.

The retrieved ghost images are also evaluated by using the SNR [24]. Figure 3 shows SNR values of the retrieved ghost images with a different number of realizations in conventional GI and the proposed TCGI, when complex and dynamic environment in Fig. 1 is studied. It is shown in Fig. 3 that SNR values of the retrieved ghost images in the proposed TCGI increase correspondingly as the number of realizations increases, and the SNR value can achieve up to 1.70. In contrast, SNR values of the retrieved ghost images in conventional GI are always close to 0 even with a large number of realizations. It is experimentally demonstrated that the theory rectified here for the GI removes effect of the physically-existing scaling factors via temporal correction, and provides a framework for the retrieval of high-resolution ghost images in various free-space wave propagation environments.
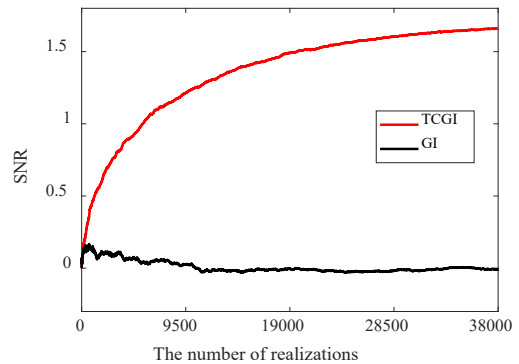

Fig. 3. Relationships between the different number of realizations and SNR values of the retrieved sample images. Conventional GI and the proposed TCGI are respectively tested, and scattering media in Fig. 1 are used.

In addition to conventional GI, modified GI reconstruction algorithms, i.e., differential GI (DGI) [22] and normalized GI (NGI) [23], also cannot retrieve any information about the sample, and experimental results are obtained (see Fig. S2 in Supplement 1). The DGI and NGI were developed to enhance quality of the retrieved ghost images. The DGI and NGI approaches totally cannot work when a scattering environment in Fig. 1 is studied.

The experimental results of DGI and NGI are similar to those obtained by using conventional GI, and no information about the sample can be retrieved in the DGI and NGI. It shows again that theoretical description about the GI based on spatially correlated beams is still incomplete. Furthermore, fundamental principle in the proposed TCGI is completely different from that in the NGI. In the NGI, the recorded single-pixel intensity value is divided by a reference value R_i, i.e., $R_i = \int I_i(\mathbf{x})d\mathbf{x}$. It can be seen that the parameters B_{ti} in Eq. (3) and R_i are different. The parameter B_{ti} denotes an interaction between the temporal carrier and intensity transmission function of the sample, and R_i denotes only the sum of each illumination pattern. The NGI was developed to enhance quality of the retrieved ghost images based on Eq. (2), and the TCGI is proposed in this study to complete a theoretical description of spatially correlated beams and establish a general framework for the GI which can give rise to applications in various free-space wave propagation environments, e.g., high-resolution imaging through complex and dynamic scattering media.

Videos, i.e., Visualization 1, Visualization 2, Visualization 3, and Visualization 4, are given to further illustrate the different GI algorithms (i.e., the GI, DGI, NGI and TCGI) in complex, dynamic and highly strong scattering environment. It is demonstrated that quality of the ghost images retrieved based on the rectified theory in the proposed TCGI is high, and conventional GI theories (i.e., the GI, DGI and NGI) cannot retrieve any information about the sample.

In addition, performance of the total variation regularization algorithm (i.e., TVAL3 [25]) through complex scattering media is also discussed (see Fig. S3 in Supplement 1). The results demonstrate advantages of the proposed TCGI method in complex scattering media.

Based on the experimental setup in Fig. 1, it is also feasible to retrieve high-resolution ghost images in the proposed TCGI when there is no turbid water tank in free space (see Fig. S4 in Supplement 1), and a comparison among different methods (i.e., GI, DGI, NGI, TVAL3 and TCGI) in free space without scattering media [26] is also conducted (see Fig. S5 in Supplement 1). It can be seen in experimental results that the proposed TCGI method also can obtain a better recovery result compared with other methods.

In recent years, deep learning has become a powerful tool for imaging through complex scattering media [27–29]. Different from the data-driven or model-driven algorithms, the proposed TCGI scheme provides a general framework for the imaging through complex scattering media. More discussions of the proposed TCGI method can be found in Section 6 of Supplement 1.

In conclusion, we have provided evidence that theoretical description about the GI based on spatially correlated beams is still incomplete and cannot work in complex scenarios, and theoretical description of temporal correction of beam correlations in the GI is completed and reported here. Characteristics of optical channel have been taken into consideration, and correlation algorithm in the GI is rectified to be applicable in a wide range of free-space wave propagation environments. The theory we rectified can establish a general framework to provide optical insights beyond the current understanding of GI, and can eliminate influence of the physically-existing scaling factors via temporal correction. By using the proposed TCGI scheme, high-resolution optical imaging through complex scattering media is realized, and quality of the recovered ghosts through complex scattering media can be enhanced effectively when the number of realizations increases. A new avenue can be opened up for the application of GI.

Disclosures. The authors declare no conflicts of interest.

Data Availability. Data underlying the results presented in this paper are not publicly available at this time but may be obtained from the authors upon reasonable request.

Supplemental document. See Supplement 1 for supporting content.

REFERENCES

1. B. I. Erkmen and J. H. Shapiro, Adv. Opt. Photon. **2**, 405 (2010).
2. J. H. Shapiro and R. W. Boyd, Quantum Inf. Process. **11**, 949 (2012).
3. D. N. Klyshko, Sov. Phys. JETP **67**, 1131 (1988).
4. D. V. Strekalov, A. V. Sergienko, D. N. Klyshko, and Y. H. Shih, Phys. Rev. Lett. **74**, 3600 (1995).
5. R. S. Bennink, S. J. Bentley, and R. W. Boyd, Phys. Rev. Lett. **89**, 113601 (2002).
6. D. Pelliccia, A. Rack, M. Scheel, V. Cantelli, and D. M. Paganin, Phys. Rev. Lett. **117**, 113902 (2016).
7. C. M. Watts, D. Shrekenhamer, J. Montoya, G. Lipworth, J. Hunt, T. Sleasman, S. Krishna, D. R. Smith, and W. J. Padilla, Nat. Photonics **8**, 605 (2014).
8. R. I. Khakimov, B. M. Henson, D. K. Shin, S. S. Hodgman, R. G. Dall, K. G. H. Baldwin, and A. G. Truscott, Nature **540**, 100 (2016).
9. S. Li, F. Cropp, K. Kabra, T.J. Lane, G. Wetzstein, P. Musumeci, and D. Ratner, Phys. Rev. Lett. **121**, 114801 (2018).
10. Y. H. He, Y. Y. Huang, Z. R. Zeng, Y. F. Li, J. H. Tan, L. M. Chen, L. A. Wu, M. F. Li, B. G. Quan, S. L. Wang, and T. J. Liang, Sci. Bull. **66**, 133 (2021).
11. A. X. Zhang, Y. H. He, L. A. Wu, L. M. Chen, and B. B. Wang, Optica **5**, 374 (2018).
12. J. H. Shapiro, Phys. Rev. A **78**, 061802(R) (2008).
13. G. Brida, M. Genovese, and I. R. Berchera, Nat. Photonics **4**, 227 (2010).
14. P. A. Morris, R. S. Aspden, J. E. C. Bell, R. W. Boyd, and M. J. Padgett, Nat. Commun. **6**, 5913 (2015).
15. A. M. Paniagua-Diaz, I. Starshynov, N. Fayard, A. Goetschy, R. Pierrat, R. Carminati, and J. Bertolotti, Optica **6**, 460 (2019).
16. B. Q. Sun, M. P. Edgar, R. Bowman, L. E. Vittert, S. Welsh, A. Bowman, and M. J. Padgett, Science **340**, 844 (2013).
17. S. Ota, R. Horisaki, Y. Kawamura, M. Ugawa, I. Sato, K. Hashimoto, R. Kamesawa, K. Setoyama, S. Yamaguchi, K. Fujiu, K. Waki, and H. Noji, Science **360**, 1246 (2018).
18. W. Chen, B. Javidi, and X. Chen, Adv. Opt. Photon. **6**, 120 (2014).
19. P. Ryczkowski, M. Barbier, A. T. Friberg, J. M. Dudley, and G. Genty, Nat. Photonics **10**, 167 (2016).
20. B. I. Erkmen, J. Opt. Soc. Am. A **29**, 782 (2012).
21. X. D. Qiu, D. K. Zhang, W. H. Zhang, and L. X. Chen, Phys. Rev. Lett. **122**, 123901 (2019).
22. F. Ferri, D. Magatti, L. A. Lugiato, and A. Gatti, Phys. Rev. Lett. **104**, 253603 (2010).
23. B. Q. Sun, S. S. Welsh, M. P. Edgar, J. H. Shapiro, and M. J. Padgett, Opt. Express **20**, 16892 (2012).
24. B. Redding, M. A. Choma, and H. Cao, Nat. Photonics **6**, 355 (2012).
25. C. Li, W. Yin, H. Jiang, and Y. Zhang, Comput. Optim. Appl. 56, 507–530 (2013).
26. Z. Cai, J. W. Chen, G. Pedrini, W. Osten, X. Liu, and X. Peng, Light Sci. Appl. **9**, 143 (2020).
27. M. Lyu, H. Wang, G. Li, S. Zheng, and G. Situ, Adv. Photon. 1, 036002 (2019).
28. E. Guo, S. Zhu, Y. Sun, L. Bai, C. Zuo, and J. Han, Opt. Express 28, 2433 (2020).
29. Y. Sun, J. Shi, L. Sun, J. Fan, and G. Zeng, Opt. Express 27, 16032 (2019).

References with titles

1. B. I. Erkmen and J. H. Shapiro, "Ghost imaging: from quantum to classical to computational," Adv. Opt. Photon. **2**, 405–450 (2010).

2. J. H. Shapiro and R. W. Boyd, "The physics of ghost imaging," Quantum Inf. Process. **11**, 949–993 (2012).

3. D. N. Klyshko, "Effect of focusing on photon correlation in parametric light scattering," Sov. Phys. JETP **67**, 1131–1135 (1988).

4. D. V. Strekalov, A. V. Sergienko, D. N. Klyshko, and Y. H. Shih, "Observation of two-photon "ghost" interference and diffraction," Phys. Rev. Lett. **74**, 3600–3603 (1995).

5. R. S. Bennink, S. J. Bentley, and R. W. Boyd, " "Two-Photon" Coincidence Imaging with a Classical Source," Phys. Rev. Lett. **89**, 113601 (2002).

6. D. Pelliccia, A. Rack, M. Scheel, V. Cantelli, and D. M. Paganin, "Experimental X-ray ghost imaging," Phys. Rev. Lett. **117**, 113902 (2016).

7. C. M. Watts, D. Shrekenhamer, J. Montoya, G. Lipworth, J. Hunt, T. Sleasman, S. Krishna, D. R. Smith, and W. J. Padilla, "Terahertz compressive imaging with metamaterial spatial light modulators," Nat. Photonics **8**, 605–609 (2014).

8. R. I. Khakimov, B. M. Henson, D. K. Shin, S. S. Hodgman, R. G. Dall, K. G. H. Baldwin, and A. G. Truscott, "Ghost imaging with atoms," Nature **540**, 100–103 (2016).

9. S. Li, F. Cropp, K. Kabra, T.J. Lane, G. Wetzstein, P. Musumeci, and D. Ratner, "Electron ghost imaging," Phys. Rev. Lett. **121**, 114801 (2018).

10. Y. H. He, Y. Y. Huang, Z. R. Zeng, Y. F. Li, J. H. Tan, L. M. Chen, L. A. Wu, M. F. Li, B. G. Quan, S. L. Wang, and T. J. Liang, "Single-pixel imaging with neutrons," Sci. Bull. **66**, 133–138 (2021).

11. A. X. Zhang, Y. H. He, L. A. Wu, L. M. Chen, and B. B. Wang, "Tabletop x-ray ghost imaging with ultra-low radiation," Optica **5**, 374–377 (2018).

12. J. H. Shapiro, "Computational ghost imaging," Phys. Rev. A **78**, 061802(R) (2008).

13. G. Brida, M. Genovese, and I. R. Berchera, "Experimental realization of sub-shot-noise quantum imaging," Nat. Photonics **4**, 227–230 (2010).

14. P. A. Morris, R. S. Aspden, J. E. C. Bell, R. W. Boyd, and M. J. Padgett, "Imaging with a small number of photons," Nat. Commun. **6**, 5913 (2015).

15. A. M. Paniagua-Diaz, I. Starshynov, N. Fayard, A. Goetschy, R. Pierrat, R. Carminati, and J. Bertolotti, "Blind ghost imaging," Optica **6**, 460–464 (2019).

16. B. Q. Sun, M. P. Edgar, R. Bowman, L. E. Vittert, S. Welsh, A. Bowman, and M. J. Padgett, "3D computational imaging with single-pixel detectors," Science **340**, 844–847 (2013).

17. S. Ota, R. Horisaki, Y. Kawamura, M. Ugawa, I. Sato, K. Hashimoto, R. Kamesawa, K. Setoyama, S. Yamaguchi, K. Fujiu, K. Waki, and H. Noji, "Ghost cytometry," Science **360**, 1246–1251 (2018).

18. W. Chen, B. Javidi, and X. Chen, "Advances in optical security systems," Adv. Opt. Photon. **6**, 120–155 (2014).

19. P. Ryczkowski, M. Barbier, A. T. Friberg, J. M. Dudley, and G. Genty, "Ghost imaging in the time domain," Nat. Photonics **10**, 167–170 (2016).

20. B. I. Erkmen, "Computational ghost imaging for remote sensing," J. Opt. Soc. Am. A **29**, 782–789 (2012).

21. X. D. Qiu, D. K. Zhang, W. H. Zhang, and L. X. Chen, "Structured-pump-enabled quantum pattern recognition," Phys. Rev. Lett. **122**, 123901 (2019).

22. F. Ferri, D. Magatti, L. A. Lugiato, and A. Gatti, "Differential ghost imaging," Phys. Rev. Lett. **104**, 253603 (2010).

23. B. Q. Sun, S. S. Welsh, M. P. Edgar, J. H. Shapiro, and M. J. Padgett, "Normalized ghost imaging," Opt. Express **20**, 16892–16901 (2012).

24. B. Redding, M. A. Choma, and H. Cao, "Speckle-free laser imaging using random laser illumination," Nat. Photonics **6**, 355–359 (2012).

25. C. Li, W. Yin, H. Jiang, and Y. Zhang, "An efficient augmented Lagrangian method with applications to total variation minimization," Comput. Optim. Appl. 56, 507–530 (2013).

26. Z. Cai, J. W. Chen, G. Pedrini, W. Osten, X. Liu, and X. Peng, "Lensless light-field imaging through diffuser encoding," Light Sci. Appl. **9**, 143 (2020).

27. M. Lyu, H. Wang, G. Li, S. Zheng, and G. Situ, "Learning-based lensless imaging through optically thick scattering media," Adv. Photon. **1**, 036002 (2019).

28. E. Guo, S. Zhu, Y. Sun, L. Bai, C. Zuo, and J. Han, "Learning-based method to reconstruct complex targets through scattering medium beyond the memory effect," Opt. Express **28**, 2433-2446 (2020).

29. Y. Sun, J. Shi, L. Sun, J. Fan, and G. Zeng, "Image reconstruction through dynamic scattering media based on deep learning," Opt. Express **27**, 16032-16046 (2019).